

ELECTROCHEMICAL CONVERSION OF CARBON DIOXIDE TO DIFFERENT HYDRO CARBONS

Rizwan Ahmed Qamar¹, Asim Mushtaq^{2,*}, Ahmed Ullah¹, Zaeem Uddin Ali¹

¹Chemical Engineering Department, ²Polymer and Petrochemical Engineering Department
NED University of Engineering & Technology, Karachi, Sindh, Pakistan

Authors e-mail address: *engrasimmushtaq@yahoo.com

ABSTRACT: The rising concentrations of CO₂ is of great concern for the world as it hurts the health and environment of people. It is known that CO₂ is the most important greenhouse gas and is a major contributor to global warming. In the past decade, efforts are being put forward for the reduction of CO₂ and rules and regulation are made. Conversion of CO₂ into Hydro Carbons is a newly born concept and is gaining attraction. The proposed work aims at developing a system which converts CO₂ into Hydro Carbons. Every industry or even a common man is releasing carbon dioxide into the environment. The research is to examine different process available that convert carbon dioxide into other products. For this purpose, simulations are done on ASPEN Plus Software check their reliability and feasibility on which different models are made for different products and optimized to get maximum output. The effect of different design parameter is also noted.

Keywords: Carbon dioxide; electrochemical; hydrocarbons; emissions; electricity; ASPEN.

1. INTRODUCTION

Carbon dioxide is a colourless, odourless gas, having a density slightly higher than air (1.98 kg/m³). Carbon dioxide molecule consists of two double covalent bonds of carbon with two oxygen atoms with formula carbon dioxide. It is a naturally occurring gas with a concentration of 4 ppm, and natural resources include volcanoes, hot springs. It is an inert gas and application includes welding, fire extinguishers, carbonated beverages. In spite of being a useful gas it is the most significant greenhouse gas, and a rapid increase in its concentration leads to global warming. Both nature and human are responsible for CO₂ emissions. Human emissions are much less than that of nature but have disturbed the equilibrium that existed for thousands of air. The major source of human CO₂ emission is burning of fossil fuel (87%). Other sources are land changes such as deforestation (9%) and industrial processing (4%) as shown in Figure 1 [1, 2].

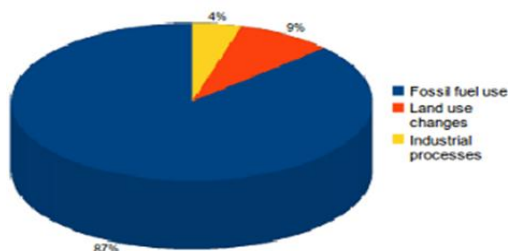


Fig. 1. Human emissions of CO₂

The fossil fuel is usually used by the electricity sector, transportation sector and industrial sector. The first two sectors produce one-third of global carbon dioxide emanations in 2019. Heat generation and electricity is the economic part that generates the highest amount of human-made carbon dioxide emanations. This sector generated 41% of fossil fuel connected CO₂ emanations in 2019. Globally, this part depends vigorously on coal, the significant carbon-intensive of fossil fuels, clarifying this area huge carbon impression [3, 4].

Practically all industrialized countries generate most of their power from the consuming of fossil fuels (about 60-90%),

except Canada and France. Figure 2 shows the IAEA's approximates of absolute ozone-depleting substance (GHG) emanations from the total power generation chains for lignite, oil, coal, flammable gas, hydroelectricity, solar photovoltaics, tidal, wind, biomass and atomic power. If there should be an occurrence of atomic power, it is significant to study total power chains and all GHGs. Some against atomic lobbyists, while concurring that atomic power creation produces no GHG emanations at the phase of generation, have fulfilled that the parity of the atomic power bind produces outflows practically identical to those from fossil fuels. GHG emanations at the phase of power age appear in the red bar sections. Appeared in the blue bar, are emanations from every single other purpose of the power chain, fuel mining, arrangement, and transport; plant development and decommissioning; the production of gear; and (on account of some renewables like hydroelectricity) the rot of natural issue. Atomic control, wind, biomass, and hydroelectricity have the most reduced full-chain emanations. The different bars for each fuel in the figure show the scope of appraisals, including future projections fusing enhancements and rotations in the fuel-to-vitality administration change process, decreases during fuel extraction and transport, and lower discharges during plant and hardware development.

The mix electricity-generating energy sources constitute 84% of worldwide power provided today from non-atomic sources. The unexpected increment in carbon dioxide discharges seen during the most recent 250 years is relied upon to proceed for a long time to come. Numerous situations have been examined, contingent upon parameters like fuel use and effectiveness. Indeed, even the most ideal situation predicts further increments in carbon dioxide levels until 2040. Huge numbers of the scenarios reason that by the centre of the 21st-century outflows of carbon dioxide ought to in any event start decrease, however, some think increment in emanations consistently. Although the different situations anticipate an enormous approximation in carbon dioxide emanations, the proposed net impact on environmental carbon dioxide focuses, later on, is to a great extent steady. All anticipate further increment in carbon dioxide levels before this present century's over, with a portion of the cases foreseeing a multiplying or in any event, trebling of the

present groupings of carbon dioxide. On the off chance that the proposed increments in ozone-depleting substance focuses are, at that point converted over into temperature changes, a worldwide temperature increment of somewhere in the range of 1 and 5.5 degrees centigrade is anticipated for 2100 [4, 5].

The normal anticipated increment in temperature is about 3 degrees centigrade over the next 100 years. This includes increment of around 1-degree centigrade because of past man-made ozone-depleting substance emanations. The measure of variety between forecasts of the various cases underlines the multifaceted nature associated with making such expectations and the enormous measure of vulnerability characteristic in environmental change models. Conferring to energy information administration “The combined carbon

dioxide emissions from China & India in2030 from coal use will be three times that of USA (China 8286 million tons of coal, India 1371 million tons of coal, USA 3226 million tons of coal)”.Other than the environmental change understandings of any innovation with clear atmosphere advantages can constrain alternatives, adaptability, and cost adequacy. The most ideal route for economic improvement – for addressing the requirements of the present without settling on the necessities of who and what is to come – lies in letting the future ages to settle on their own choices about vitality choices, and enabling all choices to contend on the stage based on cost-adequacy, ozone-depleting substance decreases, ecological wellbeing and assurance, security, and security [6, 7].

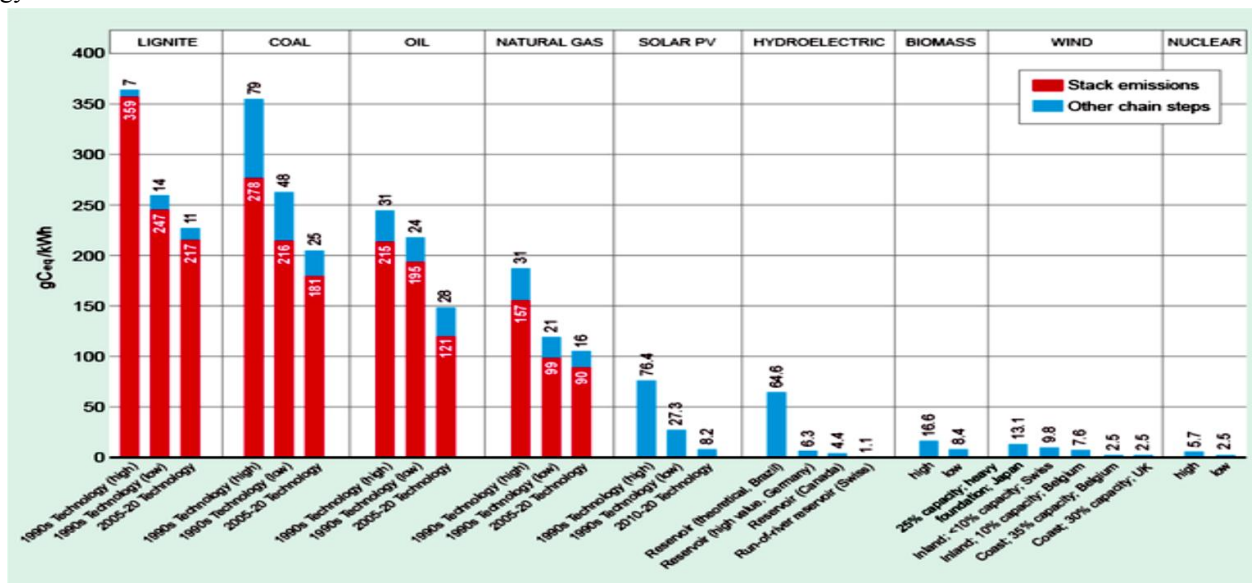
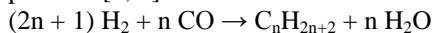


Fig. 2. CO₂ Emissions from different electric generating sources

Hydrocarbon production from Fischer Tropsch is well known and is being used for almost 50 years. The overall reaction is endothermic; the main catalysts used in this process are iron and cobalt-based FT-catalysts. Actual applications show rather limited high methane selectivity and olefin selectivity, along with severe carbon deposition. Hence, catalyst optimization is required before industrial applications are possible [8, 9].



The greater part of the work in this field has been centred on the utilization of Fischer-Tropsch catalysts intended for CO-fed frameworks. Iron-based frameworks have been the best, in view of the way that they produce lighter hydrocarbons. Then again, cobalt-based catalysts are utilized for the creation of heavier hydrocarbons in the mechanical Fischer-Tropsch process as a result of their high movement, great selectivity and predominant steadiness. In any case, they regularly present poor movement in the major carbon dioxide hydrogenation step.

Additionally, when carbon dioxide is added to a CO/H₂ stream, the hydrocarbon dispersion is firmly influenced with an adjustment in selectivity towards undesired items, for example, methane. At the point when the feed-gas is moved

to a CO/H₂ blend, cobalt frameworks tend to act as methanation catalysts with solely (for the most part >90%) methane shaped. To improve the catalyst execution, little convergences of dopants are generally added to the iron and cobalt-based impetuses (both). Advertisers regularly used with cobalt Fischer-Tropsch catalyst platinum and palladium have little impact on the item conveyance when carbon dioxide is utilized as the carbon source. Ongoing research done on this venture shows that utilization of molybdenum and sodium as advertisers to cobalt improves the specific creation of C₂₊ hydrocarbons.

Figure 3 process flow diagram of the overall process. The stream mainly consisting of carbon dioxide and H₂ is fed to reverse water gas shift reactor at high pressure (30 atm) and high temperature (1000 °C). The optimum condition for 60% conversion is 400 °C, and 0.19 atm (20 Kpa). The reaction is exothermic (H=-40 KJ/mol). The stream is then passed to the condenser where water is removed and then passed through the separator, unreacted Hydrogen is recycled back to the reactor, and the product (CO) is fed to compressor where hydrogen is also fed and heated and passed to Fischer Tropsch reactor. The overall reaction is endothermic, and the

catalyst is cobalt and Iron. The desired Hydrocarbons are obtained.

The advantages are processed cheap as compared to other processes. The process is used in a verity of industries including petroleum industry. The process is reliable and robust. The disadvantages are processed needs hydrogen stream, which results in extra cost and storage and supply. Extra precautionary safety measure is needed for hydrogen as it is a flammable substance. Photocatalytic conversion of CO₂ into hydrocarbons through thermolysis process. Solar

transformation of carbon dioxide to carbon-based fills is a promising course, which is practical through the atomistic hydrogenation of carbon dioxide particles in the semiconductor helped water-photograph parting reactors. By effortless aqueous strategy, an environmentally friendly, low-cost, nanocomposite solar energy material can be a plan in the presence-absence of carbon nanotube (CNT) and applied in fluid condition for the photochemical production of ethanol, oxalic acid and formaldehyde [10, 11].

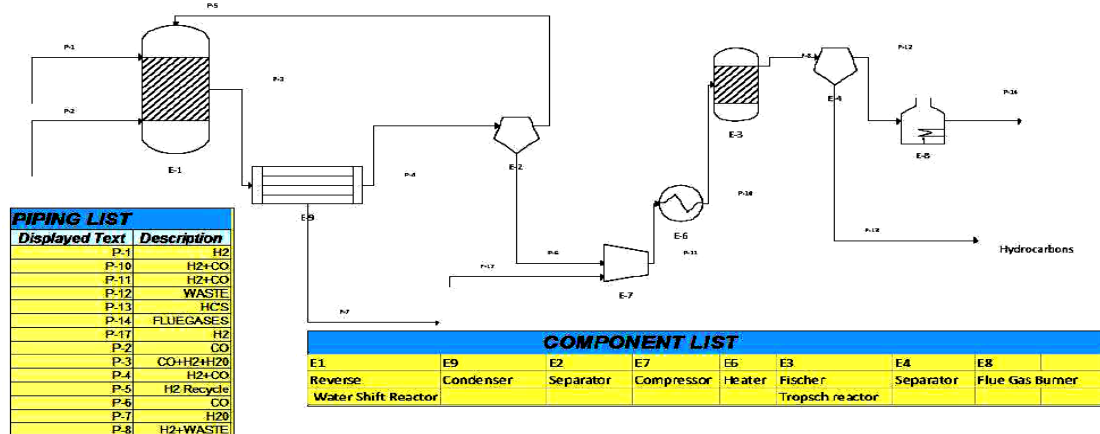


Fig. 3. Process Flow diagram of the whole Process

2. METHODOLOGY

The electrochemical conversion of CO₂ into Hydrocarbons can greatly overcome the CO₂ emissions hence reducing global warming. Electrolysis is a process in which electrical energy is utilized to perform a chemical reaction. Different Hydrocarbons can be produced at high faradic efficiency of 80-90% on various metal catalysts. Experimental studies show the effect of various electrode catalysts on the conversion performance, like copper, tin, tin oxides and Sn. It is observed that Sn has extraordinary faradic efficiency in electrochemical conversion of CO₂.

The CO₂ electrocatalytic decreases to Hydrocarbon fuels are the turnaround electrochemical procedures contrasted with the anode reactions occurring in fuel cells. CO₂ decrease changes over electrical vitality return to chemical energy deposited in the chemical bonds of fuels. The energy of carbon dioxide decrease is constantly positive at high and medium pH run, and the hypothetical possibilities are negative. Subsequently, CO₂ decrease is an electrolytic procedure that needs electrical vitality input. The potential required to electrochemically lessen CO₂ is consistently > 1.0 Volt, become sensible measures of powers, for example; ethylene, methane and so on. In a fluid electrolyte, the water is constantly decreased, and H₂ is a significant side-effect alongside CO₂ decrease. High hydrogen metals overvoltage, for example, Hg, can control H₂ production. However, it stimulates the production of formate particles (HCOO⁻) at exceptionally high over possibilities (high vitality cost). Great work has been done in this field, and many research articles are available. In this research to simulate different

available project and optimize them on a real scale. The process is thermodynamics of electrolysis. Starting of water electrolysis needs a minimum cell voltage: the reversible potential. At this potential, no losses are observed in the process [5, 12].

$$V_{rev} = -\Delta G^\circ / (n \cdot F)$$

Where *n* represents the number of electrons transferred (in case of water electrolysis), and *F* is the Faraday's constant, equal to 96487 C/mol. Conditions at which the cell operates adiabatically, this cell voltage is called the thermos neutral potential:

$$V_{th} = -\Delta H^\circ / (n \cdot F)$$

Cell voltages above the thermos neutral potential, called overpotentials, consist of an excess amount of energy and will result in heating up of the cell. Cell voltages lower than the thermos neutral potential will result in the cooling down of the cell. Heat transfer of electrolysis can be defined as the amount of heat released *Q_{rev}* and the amount of heat generated *Q_{irr}*.

$$Q_{rev} = -T\Delta S = \Delta G^\circ - \Delta H^\circ = nFV_{rev} - \Delta H^\circ$$

$$Q_{irr} = (V - V_{ref})nF$$

The total heat generated is the sum of the released and generated heat [5, 13].

$$Q = Q_{rev} + Q_{irr} = nFV - \Delta H^\circ$$

Efficiencies for electrolysis can be described from the thermos neutral (*V_{th}*) and operating voltage (*V*), which is the HHV of one mole of the product divided by the energy utilized.

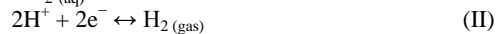
$$\epsilon = \Delta H^\circ / \Delta G^\circ = V_{th} / V$$

The ECFORM Process

The ECFORM procedure is a consistent procedure created by DNV GL, utilizing Sn as a base catalyst and changing over carbon dioxide to formate and formic acid. Change of carbon dioxide happens in an electrochemical reactor. The driving force is applied to external voltage, provided by renewable or conventional power sources.

The procedure comprises two electrodes (cathode and anode) over which the current is applied. These electrodes are set in chambers isolated by an ion-exchange membrane prohibits mass blending of the solution streaming in both chambers while permitting ions to move over and retain electrical interaction in the solution. An appropriate electrolyte alongside carbon dioxide is presented in the chamber where it interact with the cathode, and dissolved carbon dioxide in solution is changed over the products. The reaction is finished inside the anode chamber by the oxidation reaction [14, 15].

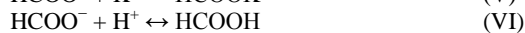
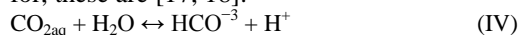
In the cathode chamber, the inlet flow is an aqueous solution of carbon dioxide gas. The aqueous carbon dioxide is at harmony with carbon dioxide gas bubbles scattered in the water at the input that is sustained on Ni, carbon dioxide is electrochemically decreased to produce HCOO^- ions, at the cathode. A few protons are also decreased to create H_2 gas. Although carbon dioxide, CO is likewise decreased, however indefinite quantities.



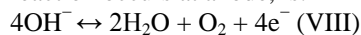
The carbon dioxide is spent in the aqueous form at the catholyte and is in harmony with the carbon dioxide in the vaporous structure which is also given by the inlet stream of saturated solution from the base of the reactor over the permeable catholyte. The H^+ ions are delivered because of hydrolysis of carbon dioxide, or transfer through the ion-exchange membrane from the anode chamber. In the cathode electrolyte chamber, because of the thin passage width and the scattered multiphase stream, blending impacts assume a significant job in the distribution of ions [15, 16].

The Faradaic proficiency is the proportion of the efficiency of the electrochemical transformation method, as it imitates

proportion of the total provided power requisite to create formate ions as indicated by the Eq. (I). Table 1 also, there are numerous other mass reactions that should be expressed for, these are [17, 18]:



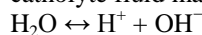
The inlet flow is either an aqueous solution of K_2SO_4 and H_2SO_4 or 1 M KOH in the anolyte chamber. The oxidation reaction occurs at anode, is:



In the anolyte, when the inlet flow stream is K_2SO_4 and H_2SO_4 , the chemical reactions happen as:



Water separation reaction happens both in the anolyte and catholyte fluid mass:



The ECFORM process is kept continuous for optimum production, as shown in Figure 4. High surface area cathodes are used. The cell dimensions are given in Table 2. Normal Operating Conditions of ECFORM process Table 3 [19, 20].

Properties of formic acid include colorless liquid with penetrating, pungent odor having a bitter taste, with melting point 8.3°C , the boiling point is 101°C , and flash point 69°C (closed cup). It is miscible with acetone, ether, methanol, ethyl acetate, and ethanol; partially soluble in toluene, benzene, xylenes. Breaks up to the degree of about 10% in benzene, toluene, and xylenes, and a lesser degree in aliphatic hydrocarbons. Miscible with water 1000000 mg/L (at 25°C) water solubility, vapor pressure 42.59 mm Hg at 25°C , may fall apart in normal storage and cause danger. Auto ignition 539°C , the substance decays on warming and contact with solid acids (sulfuric acid) delivering carbon monoxide, viscosity 1.607 mPas at 25°C and destructive to metals [1, 21].

Table 1. Mass reaction expression

Equation Number	Forward Rate	Units	Backward Rate	Units	Equilibrium Rate	Units
IV	47.6	$\text{m}^3/\text{s}/\text{mol}$	1.55E-06	$\text{m}^3/\text{s}/\text{mol}$	2.25E-08	-
V	55.05	$\text{m}^3/\text{s}/\text{mol}$	0.02	1/s	3.31E-04	m^3/mol
VI	0.54	$\text{m}^3/\text{s}/\text{mol}$	1.86	1/s	3.48	m^3/mol
VII	59.76	$\text{m}^3/\text{s}/\text{mol}$	1.00E-06	1/s	2.67	m^3/mol

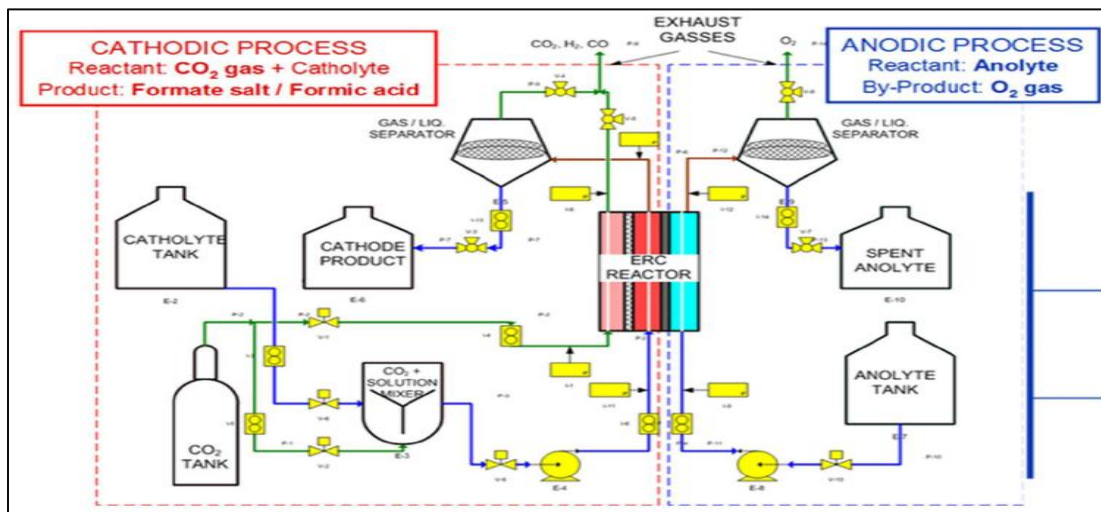


Fig. 4. Process flow diagram of ECFORM process

Table 2. Dimensions of ECFORM

Parameter	Symbol cell dimensions	Value	Unit
Cell width	W	0.033	m
Cell height	H	0.033	m
Channel length	L	0.005	m

Table 3. Normal operating conditions of ECFORM process

Operating	Symbols	Parameter	Unit
Anolyte flow rate	F_{an}	0.75×10^{-3}	l/s
Catholyte flow rate	F_{cat}	1.67×10^{-4}	l/s
Cell temperature	T	300	K
Cell pressure	P	101325	Pa
Voltage	V_{cell}	3.25 - 3.75	V
CO ₂ Molar concentration	C_{CO_2}	32	mol/m ³

3. RESULT & DISCUSSION

3.1. Simulation of Process

Simulation is done on Aspen Plus because it is a rigorous approach and friendly user interface and a wide variety of models including. The sour water solutions containing dissolved CO₂, NH₃, H₂S, and HCN, once in a while with extra solvents. The aqueous amines for gas improving water having MEA, DGA, MDEA, or DEA for the expulsion of CO₂ and H₂S. Aqueous acids or bases H₂SO₄, HBr, HCl, H₃PO₄, NaOH, HF, HNO₃, KOH, at times with extra solvents. The salt-like NaCl, KCl, CaSO₄, Na₂SO₄, CaCO₃ in solution, spend some phase with a contribution. To specify simulation for a new run under introduced layouts in the board on the left half of the new discourse box, select electrolytes. At that point, select the electrolytes with metric

unit's layout. Data for unit sets, property technique. That is pre-defined in the template are shown in Figure 5 on the right side, in the preview field. Select create to apply this template.

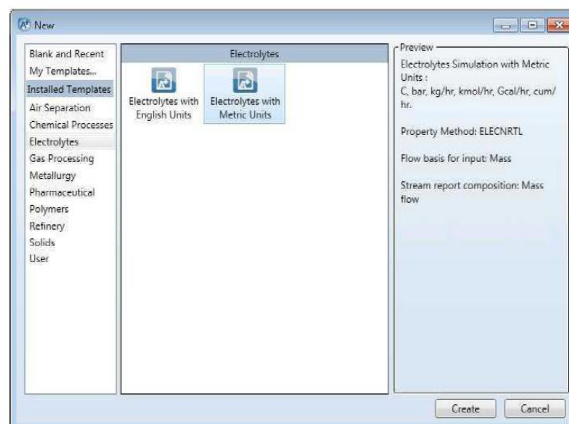


Fig. 5. Selecting the electrolyte template

The Components - Specifications sheet shows up in the workspace is appeared in Figure 6. The evident (or base) segments for this simulation are CO₂, H₂O, H₂SO₄ and HCOOH. Since, select an electrolytes format, water is now showing up on the sheet. Determine the rest of the parts by entering CO₂ and H₂O on the following two lines of the Component ID section. Aspen Plus consequently fills in the remainder of the information for this part.

The Electrolyte Wizard to describe the salts and ionic species, produced from the base parts entered on the Components Selection to create the responses that happen amongst these segments in the liquid stage. Select Elec Wizard; the Electrolyte Wizard discourse box shows up. This wizard defines automatic chemistry generation

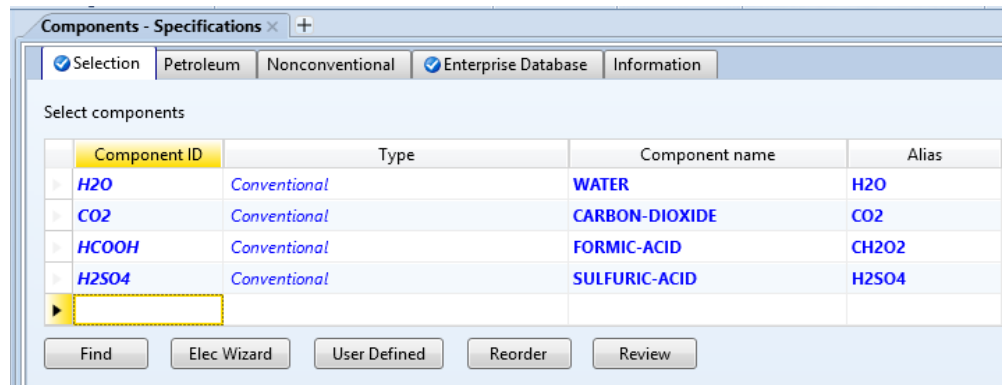


Fig. 6. Specifying components

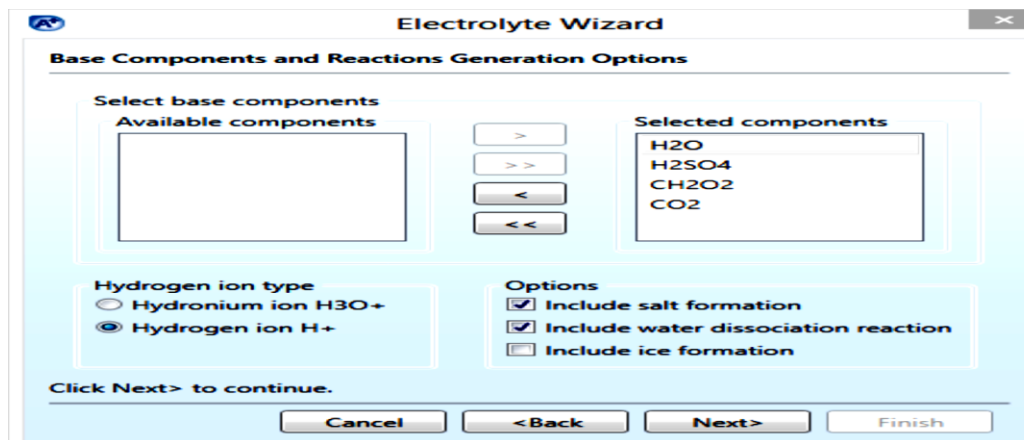


Fig. 7. The Electrolytic Wizard

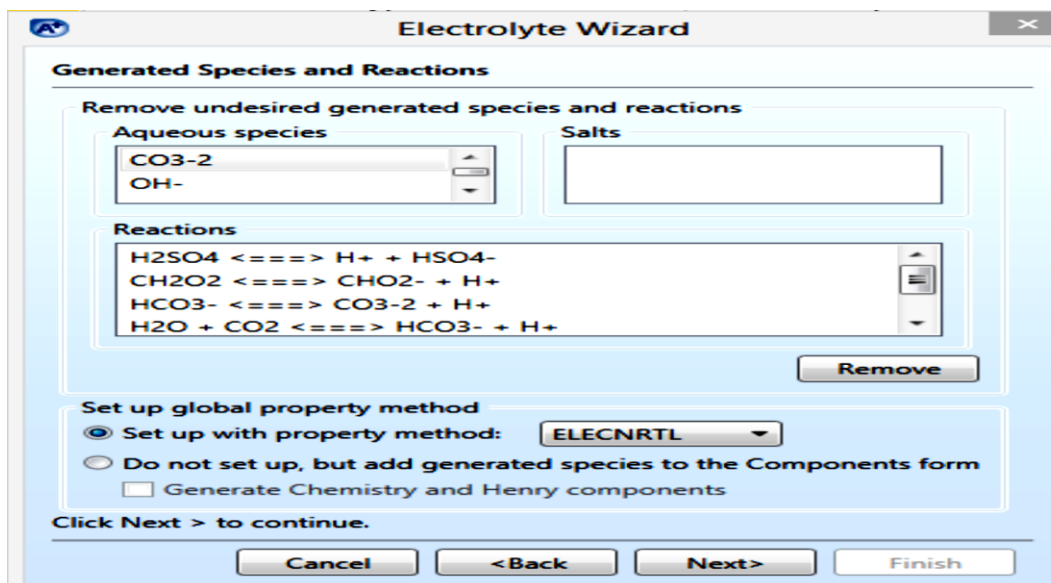


Fig. 8. Chemical reactions

The select chemistry databank and reference state area show the wizard's source of response information, base components and reactions generation options have appeared in Figure 7. There is a lot of choices for Hydrogen ion type. The default is Hydronium ion H_3O^+ . However, Hydrogen particle H^+ is also

accessible. All segments in the accessible parts segment are chosen.

Generated species and reactions appear Aspen, plus create all potential ionic reactions and salt species for the $\text{H}_2\text{O}-\text{CO}_2$ system. This section shows, various style arrows indicate the following reaction types (<====>) for salt precipitation or ionic

equilibrium and \rightleftharpoons for complete dissociation). In this process, all the reactions generated are equilibrium reactions, as shown in Figure 8.

There are two electrolyte property packages available. ENRTL-RK and ELECNRTL. ELECNRTL is used as a property package because it can speak to fluid and watery/natural electrolyte frameworks over the whole scope of electrolyte focus with an electrolyte arrangement of a single set of binary interaction parameters. ELECNRTL can

simulate fluid and watery/natural electrolyte arrange over the full scope of electrolyte focuses with an electrolyte arrangement of binary interaction specifications. Without electrolytes, the model reduces to the standard NRTL model. From the Navigation Pane, select the Review Chemistry folder, as shown in Figure 9. After review chemistry, this window will open where we can EDIT and enter new reactions per need, as shown in Figure 10.

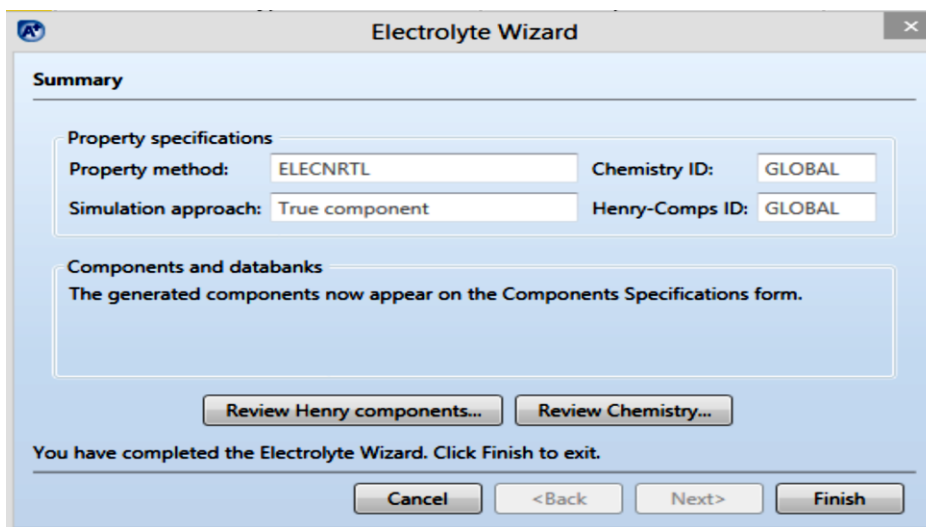


Fig. 9. Examine the generated chemistry

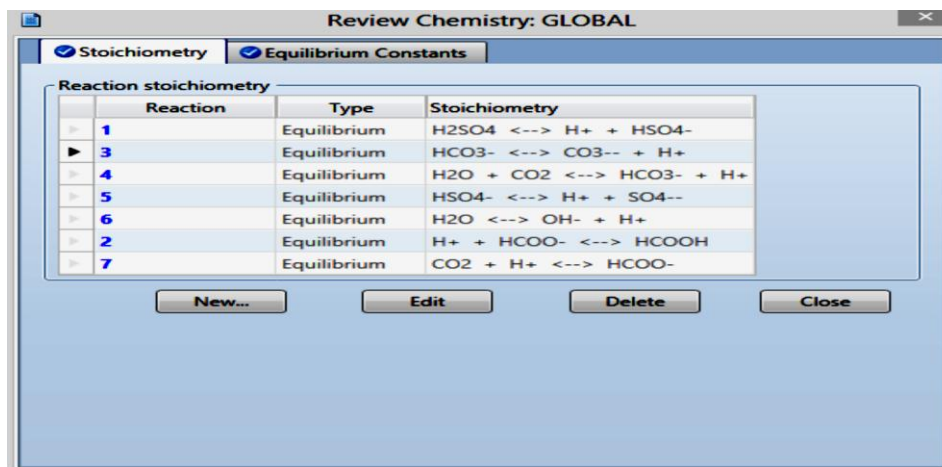


Fig. 10. Review chemistry

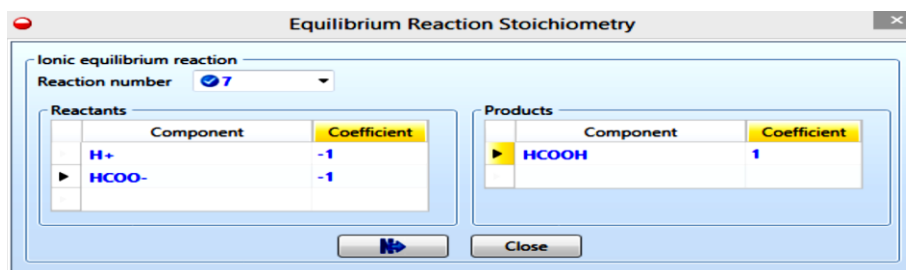


Fig. 11. Equilibrium reaction stoichiometry

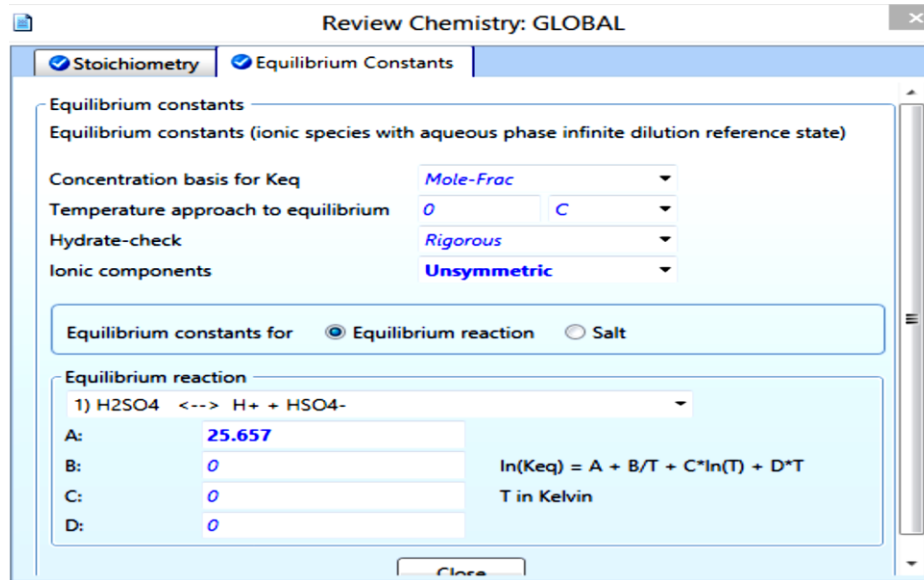


Fig. 12. Equilibrium constants

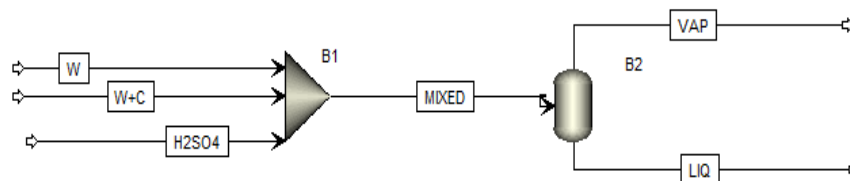


Fig. 13. Simulation flow diagram

Click the Equilibrium Constants tab to enter and view the equilibrium constant is shown in Figure 11. The reaction at equilibrium (Nernst equation), where $Q = K$ and K is the equilibrium constant for the cell reaction [17]. Then it produces zero potential difference among the electrodes, $E = 0$ gives

$$\ln K = nFE^\circ/RT$$

By the above equation, calculate equilibrium constants from standard cell potentials, as shown in Figure 12.

All input requirements are completed. Then go to the simulation tab and draw the flow sheet. Figure 13 presents the operating conditions of process flow. Three feed streams, W+C stream containing a 0.9-mole fraction of water and balance carbon dioxide, C stream consist of pure carbon dioxide & H_2SO_4 stream contains a 0.2-mole fraction of H_2SO_4 , and balanced H_2O are served to a mixer. The outlet of mixer is fed to the flash. MIXER model is used for mixer and the FLASH model for flash. Enter all stream data and run the simulation.

The status sheet shows up the result summary, representing that the simulation finished normally. The material sheet shows up, analysis the results on this sheet Figure 14.

3.2. Equilibrium Constant

The equilibrium constant is calculated by the Nernst Equation. The Nernst equation equates the decreased potential of an electrochemical response to the temperature, standard electrode potential and chemical reactions taking place in the electrolytic cell [8, 17].

$$\Delta G^\circ = -nFE^\circ$$

$$\Delta G = -nFE$$

$$\Delta G = \Delta G^\circ + RT \ln Q$$

$$-nFE = -nFE^\circ + RT \ln Q$$

$$E = E^\circ - (RT/nF) \ln Q$$

At equilibrium; $E=0$ and $Q=K$.

$$\ln k = nFE/RT$$

where; K = Equilibrium constant, n = Number of electrons = 2, F = Faradic constant = 96485 °C/mol., R = Universal Gas Constant = 8.314 J/mol K, T = Temperature=300 K, E = Electrode Potential = 1.48 J/°C. Therefore $\ln K= 114.5$.

		Units	4	5	6	
▶	To		B2			
▶	Substream: MIXED					
▶	Phase:		Mixed	Missing	Liquid	
▶	Component Mole Flow					
▶	H2O	KMOL/HR	89	0	89	
▶	CO2	KMOL/HR	1.4004e-39	0	2.3773e-40	
▶	HCOOH	KMOL/HR	0.222962	0	0.56021	
▶	H2SO4	KMOL/HR	9.0382e-17	0	3.8746e-17	
▶	H+	KMOL/HR	10.5198	0	10.4122	
▶	OH-	KMOL/HR	9.27681e-09	0	7.819e-12	
▶	HCO3-	KMOL/HR	1.2045e-43	0	9.3004e-44	
▶	HCOO-	KMOL/HR	28.777	0	28.4398	
▶	HSO4-	KMOL/HR	0.257275	0	0.0276177	
▶	CO3--	KMOL/HR	1.9407e-49	0	2.2742e-50	
▶	SO4--	KMOL/HR	19.7427	0	19.9724	
▶	Component Mass Flow					
▶	H2O	KG/HR	1603.36	0	1603.36	
▶	CO2	KG/HR	6.1632e-38	0	1.0463e-38	
▶	HCOOH	KG/HR	10.262	0	25.784	
▶	H2SO4	KG/HR	9.954e-15	0	3.9903e-15	

Fig. 14. Simulation results

The total heat energy is given by:

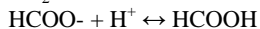
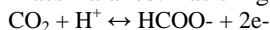
$$Q = Q_{rev} + Q_{irr}$$

$$Q = nFV - \Delta H^\circ$$

$\Delta H^\circ=0$ (From simulation results)

$$Q=675395 \text{ J}$$

Mass Balance: Basis 1 g mole of CO₂



$$n = 2.07286\text{E-}05$$

Total number of moles= n* stoichiometric moles of HCOO⁻ in equation

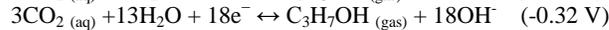
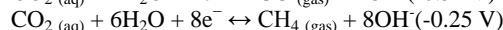
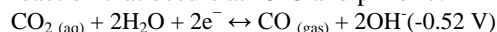
n = Coulombs/ (unsigned numeric charge on the ion * Faraday)

n = (Current in amperes * time)/ (unsigned numeric charge on the ion * Faraday)

Column1	Column2
CO ₂ (Kmol)	28
1 gmol CO ₂	2.07286E-05 Moles
so,	
28 Kmol CO ₂	0.580401099 Kmol of HCOO

Aspen Plus calculations of heat and material balance are given in Table 4. Electrochemical conversion of CO₂ to

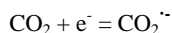
different hydrocarbons. It can be reduced to various products. The product formed depends upon the electrocatalyst, concentration of the reactants, temperature, electrode potential, electrolyte solution and material. The reaction that occurs at 25°C and pH of 7.



Reduction of carbon dioxide does not arise promptly, and for carbon dioxide decrease the applied electrolysis possibilities are negative than the equilibrium values. This is significant due to the reduction of single electron of carbon dioxide to CO₂⁻, that is all around as the initial step to activate carbon dioxide for further decrease, at - 1.90 V, because of high reorganizational energy concerning bent radical and anion linear molecule. This progression has similarly been perceived as the RDS (rate deciding advance) for carbon dioxide decrease [1, 22].

Table 4. Heat and material balance

Heat and Material Balance Table							
Stream ID		1	2	3	4	5	6
From					B1	B2	B2
To		B1	B1	B1	B2		
Phase		LIQUID	VAPOR	LIQUID	MIXED	MISSING	LIQUID
Substream: MIXED							
Mole Flow	kmol/hr						
H2O		8.000000	0.0	80.000000	89.000000	0.0	89.000000
CO2		2.8169E-28	28.000000	0.0	1.4004E-39	0.0	2.3773E-40
HCOOH		2.2678E-14	0.0	0.0	.2229619	0.0	.5602095
H2SO4		0.0	0.0	1.16433E-9	9.0382E-17	0.0	3.8746E-17
H+		3.2123E-14	0.0	20.05341	10.51976	0.0	10.41217
OH-		1.000000	0.0	4.2154E-17	9.27681E-9	0.0	7.8190E-12
HCO3-		4.7132E-20	0.0	0.0	1.2045E-43	0.0	9.3004E-44
HCOO-		1.000000	0.0	0.0	28.77704	0.0	28.43979
HSO4-		0.0	0.0	19.94659	.2572746	0.0	.0276177
CO3--		1.3858E-14	0.0	0.0	1.9407E-49	0.0	2.2742E-50
SO4--		0.0	0.0	.0534059	19.74273	0.0	19.97238
Mass Flow	kg/hr						
H2O		144.1222	0.0	1441.222	1603.360	0.0	1603.360
CO2		1.2397E-26	1232.274	0.0	6.1632E-38	0.0	1.0463E-38
HCOOH		1.0438E-12	0.0	0.0	10.26197	0.0	25.78402
H2SO4		0.0	0.0	1.14197E-7	8.8646E-15	0.0	3.8002E-15
H+		3.2360E-14	0.0	20.20160	10.59750	0.0	10.48912
OH-		17.00789	0.0	7.1696E-16	1.57779E-7	0.0	1.3298E-10
HCO3-		2.8759E-18	0.0	0.0	7.3494E-42	0.0	5.6749E-42
HCOO-		45.01829	0.0	0.0	1295.493	0.0	1280.311
HSO4-		0.0	0.0	1936.258	24.97419	0.0	2.680915
CO3--		8.3162E-13	0.0	0.0	1.1646E-47	0.0	1.3647E-48
SO4--		0.0	0.0	5.130428	1896.579	0.0	1918.641
Total Flow	kmol/hr	10.000000	28.000000	120.0534	148.5198	0.0	148.4122
Total Flow	kg/hr	206.1473	1232.274	3402.812	4841.235	0.0	4841.266
Total Flow	cum/hr	.2467014	135.2935	2.663961	97.12380	0.0	4.941900
Temperature	C	24.85000	24.85000	24.85000	168.0511		24.85000
Pressure	bar	5.000000	5.000000	5.000000	5.000000	4.000000	4.000000
Vapor Frac		0.0	1.000000	0.0	.0862830		0.0
Liquid Frac		1.000000	0.0	1.000000	.9137169		1.000000
Solid Frac		0.0	0.0	0.0	0.0		0.0
Enthalpy	kcal/mol	-70.26669	-94.09376	-80.75485	-87.74718		-89.85926
Enthalpy	kcal/kg	-3408.567	-2138.018	-2849.083	-2691.915		-2754.694
Enthalpy	Gcal/hr	-.7026669	-2.634625	-9.694895	-13.03219		-13.33621
Entropy	cal/mol-K	-44.19492	-2.563382	-44.80868	-49.51280		-54.22896
Entropy	cal/gm-K	-2.143851	-.0582457	-1.580879	-1.518957		-1.662424
Density	kmol/cum	40.53484	.2069575	45.06576	1.529180		30.03140
Density	kg/cum	835.6148	9.108159	1277.351	49.84602		979.6364
Average MW		20.61473	44.00980	28.34415	32.59657		32.62041
Liq Vol 60F	cum/hr		1.499618				0.0



It ought to be remembered that the hypothetical equilibrium potentials decline with increasing pH, following the Nernst condition. The serious issue of the change of carbon dioxide to liquid powers is the gathering of the nuclei and development of chemical bonds to change the basic carbon dioxide molecule into energetic and composite molecules.

The carbon dioxide decrease is profoundly constrained by the kinetic reaction. Taking into consideration their little balance potentials thermodynamically, the results of ethylene and methane ought to happen at a small cathodic potential than hydrogen, then dynamically this doesn't occur. Initially, carbon dioxide decrease produces formate and CO up to -1.12V, wherever hydrocarbons start to create, firstly ethylene

then methane forming. The methane arrangement displays more potential reliance, and these reactions accelerate, commanding over formate and CO at -1.35V. Hence, the primary difficulties for carbon dioxide decrease originate from both kinetics and thermodynamics.

3.3. Effect of Metal Electrodes on CO₂ Reduction

Hori's et al. has done a progression of great research on carbon dioxide decrease and discovered electrocatalytic metals could be isolated in four groups dependent on product selectivity. The first group metals consist of Pb, In, Hg, Sn, Tl, Cd and Bi. They have insignificant CO adsorption properties, high overvoltages for hydrogen, and carbon dioxide to CO₂⁻, so feeble equilibrium of CO₂⁻, final product is HCOO⁻. The second group of metals incorporate Ag, Au, and Zn, having average hydrogen overvoltages and powerless CO adsorption, as a result CO is obtained. As they can catalyse the breaking of the C-O bond in carbon dioxide but permit the CO desorb, consequently, gotten CO [1, 9].

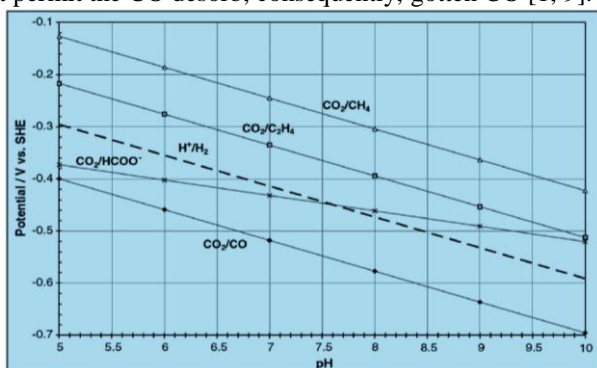


Fig. 15. Equilibrium potential versus pH for reduction of CO₂ at 25 °C

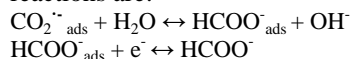
Third group of metals comprise Pt, Ni, Ti, Fe, have low hydrogen overvoltages, solid properties of CO adsorption, the primary item is H₂ since the significant response is reduction of water to H₂. The fourth group has Cu, Cu is extraordinary for carbon dioxide decrease since it can additionally respond CO to increasingly diminished species, for example, C₂H₄ and CH₄ with substantial amounts.

Azuma et al. used 32 metals for carbon dioxide decrease at comparative conditions. They indicated that Cu could diminish carbon dioxide to impressive measures of hydrocarbons CH₄ and C₂H₄, though Pt and Ni catalysts, hardly offer products in carbon dioxide decrease at ordinary pressure and temperature, however, can lessen carbon dioxide to CO or formic acid under raised pressure (60 atm). It is convincing that the existence of a limited quantity of external atoms on the surface of electrode could significantly vary the response selectivity of carbon dioxide decrease. These ad atom adjusted electrodes were arranged by overpotential or underpotential deposition procedures. For instance, at -1.44 V versus SHE, the carbonmonoxide selectivity for Cu is 69%, though Pd and Cd atom changed Cu is 0 and 82%, respectively. Reduction of carbon dioxide is widely studied, but still, carbon dioxide reduction is a topic which needs further research. The reaction mechanism that is known is discussed in Figure 15 [22].

Erring et al. explored carbon dioxide decrease polarization information in the aqueous electrolyte at Hg cathode with HCO₃⁻, and got a principle result of HCOO⁻. Reduction of

carbon dioxide on Hg is started by single electron move to form carbo CO₂⁻ at the negative potential of -1.6 V against SHE [6, 12].

The CO₂⁻ will yield a proton from water molecule at the nucleophilic C atom, producing HCOO⁻. H⁺ will not be attached with the oxide atom of CO₂⁻ as the pKa is 1.4 of CO₂⁻/CO₂H. Hori build up, constant electrode potential for HCOO⁻ creation at 2-8 pH, hence, H₂O is accepted as the proton donor from CO₂⁻ in the formate creation. HCOO⁻ is diminished to HCOO⁻ at the electrode in watery solution. The reactions are:

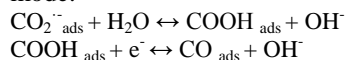


Formate could also be created legitimately by the response with adsorbed hydrogen, available as a transitional in the hydrogen evolution response,

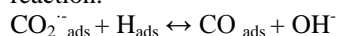


Such a response mechanism would give off an impression of being profited by CO₂⁻ being adsorbed with oxygen cooperation or present very near to the electrode. Some high H overvoltage electrodes, consist of Pb, Cd, Sn, Tl, and In, with less hydrogen adsorption, have enormous overvoltage for CO₂ reduction to CO₂⁻, and in this manner feeble stabilization of CO₂⁻. The carbon dioxide decrease in these metals continues a comparable mechanism. In non-aqueous electrolyte, carbon dioxide electrolysis on Pb helps to form oxalic acid, because of the creation of (CO₂) [12, 13].

The further pathway similarly includes the initial protonation then decrease, that is indistinguishable from step b), though the hydrogen included oxygen not carbon in CO₂⁻. This stage will happen suitable for carbon coordination adsorption mode.

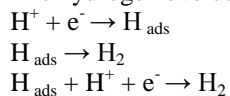


CO could be produced with adsorbed hydrogen by a direct reaction.



The electrophilic reagents which are H₂O in a watery solution, respond with the oxide atom of adsorbed CO₂⁻, producing OH⁻ and CO_{ads} in these reactions. At Au cathode, H⁺ will not participate in the formation CO, as the fractional current of CO creation isn't dependent on pH. The CO_{ads} is effectively desorbed as a gassy molecule from the electrode. The response configuration is appropriate to other metal electrodes, for example, Zn, Cu and Ag in watery solution. The arrangement of CO selectivity around concurs with electrode possibilities. This arrangement affirms the theory that CO is well-shaped from the metals electrode, which balance out CO₂⁻ strongly. Since the CO adsorption on Ag, Zn and Au surface is feeble, the fundamental product is CO. In correlation, CO will be additionally decreased to hydrocarbon on Cu electrode.

Hydrogen Evolution Reaction (HER) is the principle side response that pursues carb CO₂ on dioxide decrease in an aqueous electrolyte. The kinetics reaction of HER is reliant on pH in the acid locale and pH free in the alkaline locale. The hydrogen evolution reaction are composed as [9, 23];



3.4. Cu-Based Electrocatalysts

Low over potential, -0.9V, the faradic presents that HCOO^- and CO are both satisfactory, whereas C_2H_4 starts to increment at -1.1V, CH_4 begins at -1.2V, this show that HCOO^- and CO might be antecedents to alcohols and hydrocarbons.

In contrast, Raman spectrum and FTIR show carbon monoxide is straightly adsorbed on Cu polycrystalline electrode at -0.6V, shows that carbon monoxide is the intermediate reaction framed at Cu electrode, going about as an antecedent for more decrease to alcohols and hydrocarbons. The Cu electrode surface is surrounded by CO with inclusion >90 per cent as determined at -1.0V with and deprived of CO; this could altogether stifle hydrogen advancement response. The adsorption heat of carbon monoxide on Cu is generally -17.7 kcal/mol, more than Au, yet lower than Pt and Ni. In this manner, Cu enables productively ensuing decrease of CO to create hydrocarbons and alcohols.

As carbon monoxide has been distinguished as a fundamental reaction intermediary for the development of hydrocarbons, and was utilized to look at systems of carbon dioxide decrease on Cu. Studies show that methane formation initiates at better negative potential than C_2H_4 (-1.22 versus -1.12 V), then C_2H_4 arrangement is progressively favourable in high pH. Additionally, the Tafel incline is almost differed for the two reactions. All these show arrangement of CH_4 and C_2H_4 is over exchange reaction paths from normal beginning element CO. Further compelling, the proof of absence of a mechanism of methanol shows that the C-O bond of carbon monoxide is broke down early and reliably in the reaction.

The additional conceivable reaction pathway is over the progression of $-\text{CH}_2(\text{ads})$ with CO. As $\text{C}(\text{ads})$ is effectively decreased to $-\text{CH}_2$, two $-\text{CH}_2$ can dimerise to create C_2H_4 , or another probability, CO embeds into $-\text{CH}_2$ to shape $-\text{COCH}_2$ that is progressively over diminished to C_2H_4 . Sup to this point, despite everything we need persuaded trial information, Raman spectrum/FTIR under genuine response conditions, to without a doubt, clarify the essential strides for the perplexing CO_2 reduce to hydrocarbons. It is as quiet befuddling how hydrogen species respond with CO or CO_2^- to produce hydrocarbons on Cu electrode [1, 18].

The crystal faces impacted by Cu (100) will in general outcome in a major current proficiency for C_2H_4 at moderately low potentials; one probable clarification may be hypothesized rate-determining step. The impacted by Cu (111) lean to be polarized increasingly negative possibilities and support methane formation. The Cu (110) polarize to the most negative possibilities and produce additional 2 or 3 carbon item, for example, acidic acid. The partial product flows for ethylene and methane at polycrystalline Cu, Cu (111) Cu (110) Cu (100), and electrodes, for the most part, pursued similar styles.

The general carbon dioxide reduction needs a bigger potential, and a higher distinction in potentials was develop among the diverse crystal faces. The aftereffects of one crystal investigations exhibit the electrode composition could affect the outcomes got. Metallic nanostructures will be required to give some prospects in intentionally creating increasingly valuable crystalline; nanocube rich in (100); in

this way, enhancing the arrangement of organic molecules for long carbon chain from the reduction of carbon dioxide. Similarly, it was discovered from the reactions that no basic decision of rate confirming steps fit the info, it shows that parallel and shifting components work, modifying conceivably electrolyte and electrode preparation compositions may transform the mechanisms.

Cu based composites have been analyzed for reduction of carbon dioxide. The adjustment can be because of variations in the electronic structure and alteration in the characteristics of crystallographic surface, comprising the presentation of dislocations and opportunities, prompting significant changes in the reaction rates and products distributions. Cu-Fe and Cu-Ni compounds, framed by in-situ deposition in carbon dioxide decrease, slowly drop C_2H_4 and CH_4 give together with expanded H_2 development with the ascent of Fe or Ni inclusion on the Cu surface [1, 13].

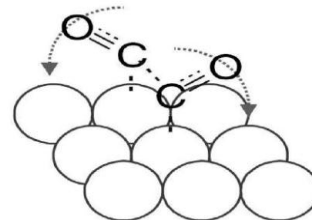


Fig.16. Mechanism on Cu for the catalysis of C_2H_4

A Cu-Cd electrode created C_2H_4 and CH_4 . This mechanism slowly fallen with the expansion of Cd inclusion. However, CO development expanded. Watanabe et al. inspect numerous Cu-based compounds; Cu-Cd, Cu-Sn, Cu-Ni, Cu-Zn, Cu-Pb, and concluded the principal items are HCOO^- and CO. The Cu-Au compound electrodes surface recommended this surface significantly smothers the production of alcohols and hydrocarbons, prompting the improvement of CO formation as appeared in Figure 16.

A magnificent option in contrast to the reduction of carbon dioxide in the aqueous electrolyte is the utilization of SPE and GDEs with anion and cation interchange membrane for a ceaseless carbon dioxide decrease framework which could empower extensive addition of mass transfer of carbon dioxide. For fuel cell innovation GDE is a permeable complex electrode formed, for the most part made out of carbon black and Teflon bonded catalyst molecules. Solid polymer electrolyte membrane with gas diffusion electrode will give gas stage electrolysis of carbon dioxide.

3.5. Economic Analysis of ECFORM Process

Formic acid is, for the most part, utilized in the animal feed market and leather tanning, and the request is developing for the pharmaceutical along with biofuel market. Significant chemical organizations, for example, BASF are growing new utilizes for formic acid in hydrogen storage and fuel cells, making it an appealing chemical. The electrochemical decrease of CO_2 to formic acid has a few points of interest over different pathways for reusing CO_2 and consolidating sustainable power source in the chemical value chain. The procedure can be performed at mild conditions (ambient pressure and room-temperature); generally synthetic utilization can be diminished to wastewater by reusing the supporting electrolytes; procedure can be driven by

sustainable power source; broad research has prompted high selectivity, minimal effort, heterogeneous catalyst; and procedure comprises of modular, compact and simple to scale-up uses of the electrolytic cells. As referenced previously, the electrochemical decrease of CO₂ to formic acid has a few points of interest over other reuse pathways. High selectivity, minimal effort, heterogeneous catalysts are accessible; the procedure can be worked at ambient pressure and room temperature [12, 21].

At first, high current densities to obtain high product generation limit the reactor size and ultimately limit the capital costs. Secondly, the used catalyst should guarantee a high Faradic efficiency to reduce the specific electricity consumption of the process. Further, a long electrode lifetime can be of importance to reduce the operational cost and allow for continuous operation. Apart from the energetic requirements, the process should also provide high product selectivity, avoid additional CO₂ generation, and guarantee long-term stable operation. To estimate the economics of the electrochemical reduction of CO₂ to formic acid is a simplified simulation of the process is modelled, it is assumed that 100% selectivity for formic acid is obtained.

The general assumptions made for the analysis of the electrochemical reduction process are given in Table 5 CO₂ be assumed to be bought 3800 PKR/ton and electricity price 14 PKR/KWh is taken as an average Electricity price

Table 5. General Cost assumptions

Quantity	Rate (PKR)*
Cost of CO ₂ Capture (PKR/Kg)	3.8
Cost of Water (PKR /L)	5
Electricity (PKR/KWh)	14
Electrode Detrition Cost (PKR/kgph)	15
H ₂ SO ₄ Cost (PKR /Kg) from Lmex	20

Key economic results for the electrochemical reduction process simulation are shown in Table 6.

Table 6. Economic results for ECFORM process

Components	Rate (PKR)*
Formic acid (Pkr/kg) Tufail Chemicals	94
Cost of CO ₂ capture (PKR/kg)	3.8
Energy Required (kwh/kg)	56
Cost of Electricity (PKR/kwh)	14
Operating cost/Variable Cost	100
Capital cost (PKR)	100000

CONCLUSION

The modelled production cost of simulation of electrochemical reduction of CO₂ is approximately 100 PKR per Kg of formic acid. This is considerably higher than the actual market value for formic acid, which is 94 PKR by Tufail Chemicals. The main cost contributors to the production of formic acid are the electricity and capital cost. Feedstock and electrode cost constitute only 2.5 % of the operational expenditures and have only a small influence on the production cost. Taking in mind the current selling price for formic acid, the electrochemical reduction of CO₂ to formic acid with renewable energy would not be feasible, but we can make it feasible by getting some favour from government as well as industry producing carbon dioxide. In

case a carbon credit would be taken into account, the price gap between the renewable and conventional Formic acid price can be reduced. The gap can be reduced by getting electricity directly on the rate of production of electricity from coal power plant which is 10 PKR and by bulk purchasing of other materials which make the process feasible and commercial.

ACKNOWLEDGEMENT

The authors would like to acknowledge the Department of Chemical Engineering and Department of Polymer and Petrochemical Engineering, NED University of Engineering & Technology, Karachi, Pakistan for supporting in this research work

NOMENCLATURE

Symbols	Units	Description
A _{bed}	cm ²	Cross-sectional area of catalyst bed
a _{cat}	cm ² /cm ³	Surface area per unit volume of catalyst
c	cm/s	Speed of light
C _i	moles/cm ³	Concentration of terminal species i
C _{is}	moles/cm ³	Concentration of terminal species i at catalyst surface
C _{ib}	moles/cm ³	Bulk concentration of terminal species i
D _e	m ² /s	Bulk or Knudsen diffusivity
d _p	cm	Catalyst particle diameter
D _g	m ² /s	Gas diffusivity
D _{AB}	kcal/mol	Bond dissociation energy
E	kcal/mol	Activation energy
E _e	kcal/mol	Electrical energy of the ground state
F _i	Moles/s	Molar flow rate of terminal species i
G _o	kJ/mol	Standard Gibbs free energy
ΔG	kJ/mol	Gibbs free energy change
h	J·s	Planck’s constant
ΔH _{rxno}	kcal/mol	Standard heat of reaction
ΔH _{of}	kcal/mol	Standard heat of formation
ΔH	kcal/mol	Enthalpy change
ΔH _{rxn}	kcal/mol	Heat of reaction
h _T	W/m ² ·K	Heat transfer coefficient
I _{ik}	-	Intermediate species k
k	s ⁻¹ or Pa ⁻¹ s ⁻¹	Rate constant
k _p	s ⁻¹ or Pa ⁻¹ s ⁻¹	Forward rate constant of elementary reaction step p
k _{rp}	s ⁻¹ or Pa ⁻¹ s ⁻¹	Reverse rate constant of elementary reaction step p
K _p	-	Equilibrium constant of elementary reaction step p
k _B	J/K	Boltzmann constant
K	-	Equilibrium constant of the overall reaction
K _t	J/K·m·s	Thermal conductivity
k _{app}	s ⁻¹ or Pa ⁻¹ s ⁻¹	Apparent rate constant
k _c	m/s	Mass transfer coefficient
L _{bed}	cm	Length of catalyst bed

m	kg	Mass of a molecule
m_{cat}	g	Mass of catalyst
N_A	molecules/mole	Avagadros number
n_i	mol/cm^3	Concentration of specie i
n	-	Number of terminal species
N_i	moles	Moles of terminal species i
P_i	Pa	Partial pressure of species i
Q_A	kcal/mol	Atomic binding energy
r_ρ	s^{-1} or $\text{Pa}^{-1}\text{s}^{-1}$	Rate of elementary reaction step ρ
r_p	s^{-1} or $\text{Pa}^{-1}\text{s}^{-1}$	Forward rate of elementary reaction step ρ
r_{rp}	s^{-1} or $\text{Pa}^{-1}\text{s}^{-1}$	Reverse rate of elementary reaction step ρ
r_{OR}	s^{-1} or $\text{Pa}^{-1}\text{s}^{-1}$	Overall reaction rate
R_{gas}	$\text{kJ}/\text{mol}\cdot\text{K}$	Gas constant
R	cm	Catalyst particle radius
S_o	$\text{kJ}/\text{mol}\cdot\text{K}$	Standard entropy
ΔS	$\text{kJ}/\text{mol}\cdot\text{K}$	Entropy change
S_i	cm^2/g	Active catalyst surface area
S	-	Active surface site
t	sec	Reaction time
T	K	Reaction temperature
T_s	K	Temperature of catalyst surface
U	cm/s	Velocity of particle
V	cm^3	Volume of gas in bed
v	cm^3/s	Volumetric flow rate of gas
X_i	-	Conversion of species i
x_i	-	Mole fraction of species i
ϵ	-	Porosity factor
μ	$\text{kg}/\text{m}\cdot\text{s}$	Fluid viscosity
μ	kJ/mol	Chemical potential of species
ϕ	-	Void fraction of catalyst bed
ρ_{cat}	g/cm^3	Catalyst density
ρ_b	g/cm^3	Bulk density of catalyst
ρ_f	g/cm^3	Fluid density
τ	s	Residence time

Abbreviations

ads = Adsorption, AFC = Alkaline fuel cell, ATR = Autothermal reforming, CSTR = Continuously stirred tank reactor, CFD = Computational fluid dynamics, CNT = Carbon nano tubes, CPOX = Catalytic partial oxidation, des = Desorption, HTS = High temperature shift, LDHs = Layered double hydroxides, LTS = Low temperature shift, MWCNT = Multi walled carbon nanotubes, OR = Overall reaction, PBR = Packed bed reactor, PEM = Polymer electrolyte membrane, PFR = Plug-flow reactor, PTFE = Polytetrafluoro-Ethylene, RLS = Rate limiting step, RR = Reaction route, SHE = Standard hydrogen electrode, SOFC = Solid oxide fuel cell, SR = Steam reforming, SS = Stainless steel, STP = Standard temperature and pressure, WGS = Water-gas shift, XRD = X-ray diffraction.

REFERENCES

[1] Ma, M., Djanashvili, K. and Smith, W.A., "Controllable Hydrocarbon Formation from the Electrochemical Reduction of CO_2 over Cu Nanowire Arrays", *Angew Chem Int Ed Engl*, **55** (23): 6680-6684 (2016).

- [2] Gonçalves, M.R., Gomes, A., Condeço, J., Fernandes, T.R.C., Pardal, T., Sequeira, C.A.C. and Branco, J.B., "Electrochemical conversion of CO_2 to C_2 hydrocarbons using different ex situ copper electrodeposits", *Electrochimica Acta*, **102** 388-392 (2013).
- [3] Roy, S.C., Varghese, O.K., Paulose, M. and Grimes, C.A., "Toward Solar Fuels: Photocatalytic Conversion of Carbon Dioxide to Hydrocarbons", *ACS Nano*, **4** (3): 1259-1278 (2010).
- [4] Peterson, A.A., Abild-Pedersen, F., Studt, F., Rossmeisl, J. and Nørskov, J.K., "How copper catalyzes the electroreduction of carbon dioxide into hydrocarbon fuels", *Energy & Environmental Science*, **3** 1311-1315 (2010).
- [5] Zangeneh, F.T., Sahebdehfar, S. and Ravanchi, M.T., "Conversion of carbon dioxide to valuable petrochemicals: An approach to clean development mechanism", *Journal of Natural Gas Chemistry*, **20** (3): 219-231 (2011).
- [6] Graves, C., Ebbesen, S.D., Mogensen, M. and Lackner, K.S., "Sustainable hydrocarbon fuels by recycling CO_2 and H_2O with renewable or nuclear energy", *Renewable and Sustainable Energy Reviews*, **15** (1): 1-23 (2011).
- [7] Gonçalves, M.R., Gomes, A., Condeço, J., Fernandes, R., Pardal, T., Sequeira, C.A.C. and Branco, J.B., "Selective electrochemical conversion of CO_2 to C_2 hydrocarbons", *Energy Conversion and Management*, **51** (1): 30-32 (2010).
- [8] Weng, Z., Jiang, J., Wu, Y., Wu, Z., Guo, X., Materna, K.L., Liu, W., Batista, V.S., Brudvig, G.W. and Wang, H., "Electrochemical CO_2 Reduction to Hydrocarbons on a Heterogeneous Molecular Cu Catalyst in Aqueous Solution", *J Am Chem Soc*, **138** (26): 8076-8079 (2016).
- [9] Tu, W., Zhou, Y. and Zou, Z., "Photocatalytic conversion of CO_2 into renewable hydrocarbon fuels: state-of-the-art accomplishment, challenges, and prospects", *Adv Mater*, **26** (27): 4607-4626 (2014).
- [10] Chang, C.-C., "A multivariate causality test of carbon dioxide emissions, energy consumption and economic growth in China", *Applied Energy*, **87** (11): 3533-3537 (2010).
- [11] Lean, H.H. and Smyth, R., "CO₂ emissions, electricity consumption and output in ASEAN", *Applied Energy*, **87** (6): 1858-1864 (2010).
- [12] Bhowan, A.S. and Freeman, B.C., "Analysis and status of post-combustion carbon dioxide capture technologies", *Environmental Science & Technology*, **45** (20): 8624-8632 (2011).
- [13] Hu, B., Guild, C. and Suib, S.L., "Thermal, electrochemical, and photochemical conversion of CO_2 to fuels and value-added products", *Journal of CO₂ Utilization*, **1** 18-27 (2013).
- [14] Taheri Najafabadi, A., "CO₂ chemical conversion to useful products: An engineering insight to the latest advances toward sustainability", *International Journal of Energy Research*, **37** (6): 485-499 (2013).
- [15] van Santen, R.A., Markvoort, A.J., Filot, I.A., Ghouri, M.M. and Hensen, E.J., "Mechanism and microkinetics

- of the Fischer-Tropsch reaction", *Phys Chem Chem Phys*, **15** (40): 17038-17063 (2013).
- [16] van Santen, R.A., Ghouri, M.M., Shetty, S. and Hensen, E.M.H., "Structure sensitivity of the Fischer-Tropsch reaction; molecular kinetics simulations", *Catalysis Science & Technology*, **1** (6): 891 (2011).
- [17] Huang, C.-H. and Tan, C.-S., "A Review: CO₂ Utilization", *Aerosol and Air Quality Research*, **14** (2): 480-499 (2014).
- [18] Li, Q., Zheng, C., Shirazi, A., Bany Mousa, O., Moscia, F., Scott, J.A. and Taylor, R.A., "Design and analysis of a medium-temperature, concentrated solar thermal collector for air-conditioning applications", *Applied Energy*, **190** 1159-1173 (2017).
- [19] Van-Dal, É.S. and Bouallou, C., "CO₂ Abatement Through a Methanol Production Process", *Chemical Engineering Transactions*, **29** 463-468 (2012).
- [20] Schouten, K.J.P., Kwon, Y., van der Ham, C.J.M., Qin, Z. and Koper, M.T.M., "A new mechanism for the selectivity to C₁ and C₂ species in the electrochemical reduction of carbon dioxide on copper electrodes", *Chemical Science*, **2** (10): 1902 (2011).
- [21] Aeshala, L.M., Rahman, S.U. and Verma, A., "Effect of solid polymer electrolyte on electrochemical reduction of CO₂", *Separation and Purification Technology*, **94** 131-137 (2012).
- [22] Jhong, H.-R.M., Ma, S. and Kenis, P.J.A., "Electrochemical conversion of CO₂ to useful chemicals: current status, remaining challenges, and future opportunities", *Current Opinion in Chemical Engineering*, **2** (2): 191-199 (2013).
- [23] Sun, H. and Wang, S., "Research Advances in the Synthesis of Nanocarbon-Based Photocatalysts and Their Applications for Photocatalytic Conversion of Carbon Dioxide to Hydrocarbon Fuels", *Energy & Fuels*, **28** (1): 22-36 (2013).